BAND GAP DETERMINATION OF NOVEL PbS-NiO-CdO HETEROJUNCTION THIN FILM FOR POSSIBLE SOLAR ENERGY APPLICATIONS

C. AUGUSTINE[a,b*], M. N. NNABUCHI[a]
[a]*Department of Industrial Physics, Ebonyi State University, Abakaliki, Ebonyi State, Nigeria*
[b]*Department of Physics, Federal University Ndufu-Alike Ikwo, Ebonyii State, Nigeria*

We report herein a simple, low cost and scalable fabrication of Novel PbS-NiO-CdO Heterojunction core-shell thin film using chemical bath deposition. The XRD results show that the film consisted of more than one peak depicting the polycrystalline nature of PbS-NiO-CdO films. The average grain size increased with increasing annealing temperatures. This is in accordance with the SEM results where the aggregate size increased appreciably with annealing temperature. From the morphology of the films, it was observed that at higher annealing temperature, the uniformity of the crystal tends to increase. There was no cracks in the magnification image which accounts for the high mechanical stability of the film. The high solar absorbance displayed by the film could be used as spectrally selective coating for solar thermal applications. Solar collectors for heating fluids require increasing the reception area of the solar radiation, and/or to increase the absorbance of the surface coating in order to improve thermal efficiency. The dependence of band gap on annealing temperature was particularly investigated. The band gap showed considerable variation with annealing temperatures with values suitable for solar photovoltaic application.

1. Introduction

Photovoltaic (PV) is the cleanest and most direct and efficient mode of solar energy conversion to electrical power [1]. Photovoltaic devices therefore provide the convenient means of producing electricity to augment conventional generating systems since they possess the advantage of being mobile, silent and can be mounted on rooftops with no waste products. Photovoltaic energy not only can help meet the growing worldwide demand for electricity, but it can do so without incurring the high economic and environmental costs of burning fossil fuels and installing power lines. It is the most attractive non-conventional energy source of proven reliability from the micro to the megawatt level. PV technology needed only a simple solid state device for direct room temperature conversion of abundant solar light into electricity. Photovoltaic systems are modular, and so their electrical power output can be engineered for virtually any application, from low-powered consumer uses-wristwatches, calculators and small battery chargers-to energy-significant requirements such as generating power at electric utility central stations.

Energy conversion in solar modules consists of electron-hole pairs creation in semiconductors by the absorption of light and separation of electrons and holes by an internally generated electric field. When two terminals of such semiconductor is connected externally, charge carries are collected by electrodes giving rise to a photocurrent [2, 3]. The spectrum of solar light energy spreads from the ultra violet region (300nm) to the infra-red region (3000nm). When a photon of energy, $h\upsilon$, smaller than the band gap of a semiconductor material is impinged on such material, the light is transmitted through the material. On the other hand, when the photon energy is larger than the band gap, electrons in the valance band are excited to the conduction band

---

[*]Corresponding author: emmyaustine2003@yahoo.com

thereby creating an electron-hole pair. The use of heterojunction (HJ) with large band gap window material and a small band-gap absorber material is a means to reduce the surface recombination loss that might otherwise dominate in direct band gap materials. Thus the use of heterojunctions expands the semiconductor material possibilities for solar photo voltaic application.

There are many studies on the synthesis of core-shell thin films using chemical bath deposition technique. Chemical bath deposition of composites, TiO_2/Fe_2O_3 [4], TiO_2/CoO [5], TiO_2/Cu_2O [6], PbS/CdS [7], TiO_2/CuO [8], ZnS/ZnO [9] have been reported. In this study, we contribute by successfully depositing novel PbS-NiO-CdO core-shell thin film using chemical bath deposition technique.

2. Experimental

The solution growth technique was used to deposit PbS/NiO/CdO core-shell thin films. First, PbS film was deposited with a chemical bath made of 5mls of 0.2M $Pb(NO_3)_2$, 5mls of 1M SC $(NH_2)_2$, 5mls of 1M NaoH and 35mls of distilled water put in that order in 50ml cleaned and dried beaker. The deposition took place at room temperature for 50 minutes. Secondly, PbS/NiO core-shell was deposited by inserting the already formed PbS into a mixture containing 10mls of 0.2M-1M $NiSO_4$, 5mls of 100% NH_3 and 27mls of distilled water into 50ml beaker. Deposition was allowed to proceed at temperature of 353K for 1 hr. To obtain the PbS/NiO/CdO core-shell, the PbS/NiO already formed (core) was inserted in a mixture containing 10mls of 0.2M-1M $CdSO_4$, 10mls of 1M SC $(NH_2)_2$, 5mls of 100% NH_3 and 30mls of distilled water into 50ml beaker. Deposition was allowed to proceed at temperature of 353K for 1 hr. Prior to the deposition, the slides were thoroughly cleaned before dipping into the reaction bath. To do this, the substrates were degreased by dipping them in concentrated hydrochloric acid. They were removed after 24 hours and dipped in cold detergent solution where they were subjected to scrubbing with soft rubber sponge. Thereafter the substrates were rinsed in distilled water and drip dried in air. The degreased, cleaned surface has the advantage of providing nucleation centers for the growth of the films, hence, yielding highly adhesive and uniformly deposited films. The substrates were dipped vertically into the center of the reaction baths in such a way that they did not touch the bottom or walls of the bath containers. Several variations of the bath constitutions of each compound whose films were to be deposited was employed. For a chosen standard reaction bath for such a compound the substrates was allowed to stay in the bath for different dip times. This is to allow the growth condition to be optimized and the baths standardized. After deposition, the films were washed in distilled water and drip dried in air after which two of them was annealed at different temperature while one was left un-annealed to serve as the control.

Thermo scientific GENESYS 10S model UV-VIS spectrophotometer was used to determine the absorbance in the wavelength range of 300-1000 nm from which the Transmittance T, Reflectance R, the Absorption coefficient α, the Band gap E_g, Extinction coefficient k and Refractive index n were estimated. The crystal phase analysis of the deposited film was carried out at room temperature with an X-ray diffractometer (Rigaku Ultima IV model), using gracing incident at 30 mA, 40 KV with CuKα radiation of wavelength λ=0.15406nm. Scanning Electron Microscope (Tescan model) was used to observe the morphology of the deposited core-shell thin films. Four point probe (Keithley model) was used to measure the voltage and current of the film samples. Rutherford backscattering (RBS) was used to determine the elemental composition, depth profile and thickness of the films by Proton Induced X-ray Emission (PIXE) scans on the samples from a Tandem Accelerator Model 55DH 1.7MV Pellaton.

3. Results and discussion

The elemental composition and chemical states of PbS-NiO-CdO core-shell thin film was analysed by Rutherford Backscattering (RSB). The results are shown in Fig.1. From the film

composition presented in table 1, we can deduce that thin film of deposited PbS-NiO-CdO in this work has no impurity content.

Table 1. Percentage composition of PbS-NiO-CdO from RBS analysis

Sample	Pb	Cd	Ni	Fe	Ca	K	S	Si	Al	Na	O
Glass Slide	-	-	-	0.30	6.00	3.50	-	34.00	5.20	25.00	26.00
PbS-NiO-CdO	31.47	77.04	17.70	-	-	-	68.53	-	-	-	22.96
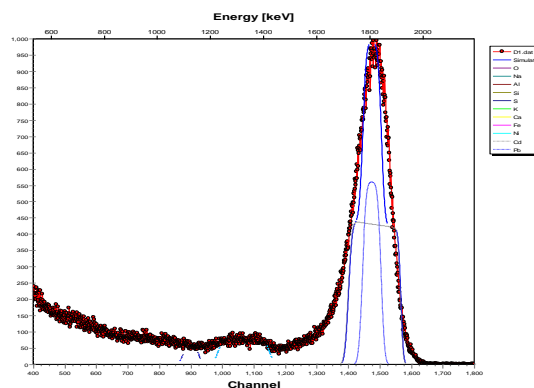
Fig. 1. RBS micro graph of PbS-NiO-CdO core-shell thin film

Fig. 2a–c display the XRD patterns of the PbS-NiO-CdO film. The XRD patterns show three marked Bragg reflections centered at approximately 26°C, 30°C and 43°C. However, a weak reflection occurred at approximately 62°C. Thermal annealing clearly affected the structural properties of the deposited films as seen in the XRD patterns presented in figure 2a, 2b and 2c for as-deposited, thermally annealed at 473K and 673K respectively. The peaks became more intense with increase in annealing temperatures. The average grain size of the deposited film samples are 97.59nm, 117.15nm and 127.96nm for as-deposited, thermally annealed at 473K and 673K respectively.
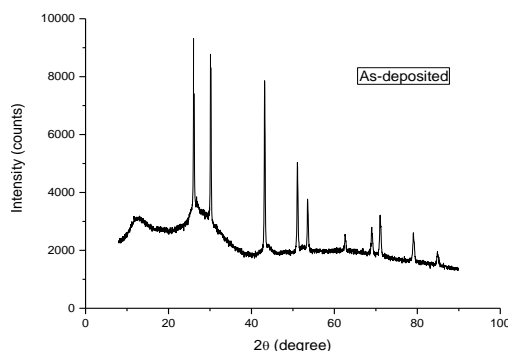
Fig. 2a XRD diffractogram of PbS-NiO-CdO as deposited

Peak broadening has been observed in the recorded diffraction patterns, which shows the formation of polycrystalline thin films. At higher temperature, both the micro strain and the dislocation density are minimum, which reveals the reduction in the concentration of the lattice imperfections leading to preferred orientations.
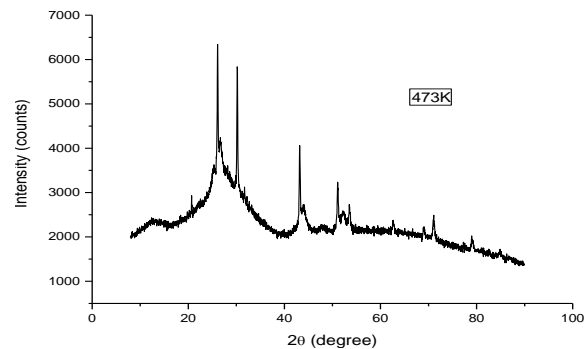
Fig. 2b. XRD diffractogram of PbS-NiO-CdO at 473K
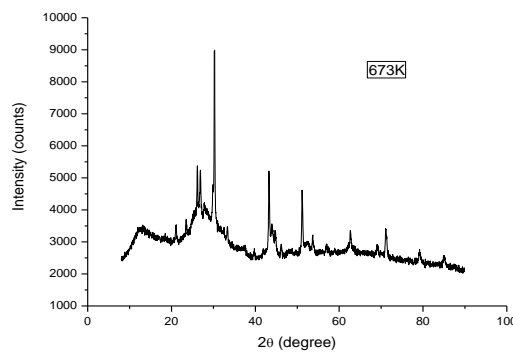
Fig. 2c: XRD diffractogram of PbS-NiO-CdO at 673K

Scanning electron microscopes is a versatile technique for studying microstructure of thin film. The surface morphologies of PbS-NiO-CdO core-shell are shown in fig. 3a-b. It can also be observed that at higher annealing temperature, the uniformity of the crystal tends to increase. No cracks are found in the magnification image which accounts for the high mechanical stability of the film. The surface morphology (Figure 3(b)) represents a denser structure with homogeneously distributed large grains compared to Fig. 3a, a continuous and well-defined grain boundaries.
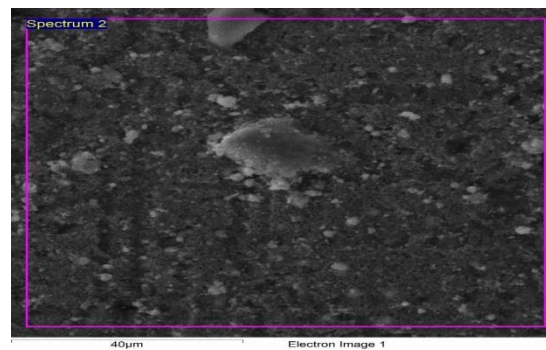
Fig. 3a: SEM image of PbS-NiO-CdO as deposited
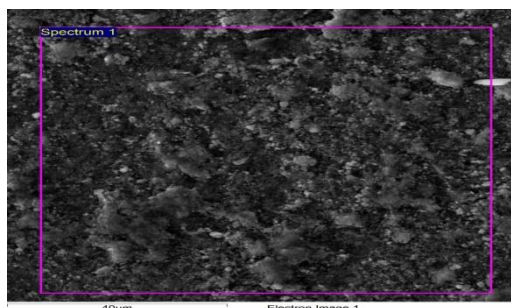
Fig. 3b: SEM image of PbS-NiO-CdO at 673K

Fig. 4 shows the graph of absorbance as a function of wavelength. It can be observed that the absorption was constant with increasing wavelength in the UV region for the as -deposited and annealed at 473K with a decrease in the visible region and sharp decrease in the near infrared region, whereas the annealed at 673K maintained constant absorbance in the UV-VIS with a sharp decrease in the near IR region. Optical absorption continuously decreases with wavelength in the near infrared through visible region due to the increase of scattering loss at the surface. The PbS-NiO-CdO sample shows maximum absorbance of 4 at a wavelength of 300-550nm for as deposited. The absorbance decrease as the wavelength increases and attains 1.174 at a wavelength of 1000nm. The annealed at 473K showed maximum of 4 at a wavelength of 300-650nm and decreases to a value of 1.619 corresponding to 1000nm wavelength. The annealed at 673K has a maximum of 4 in the wavelength range 300-700nm with minimum value of 1.846 at 1000nm.
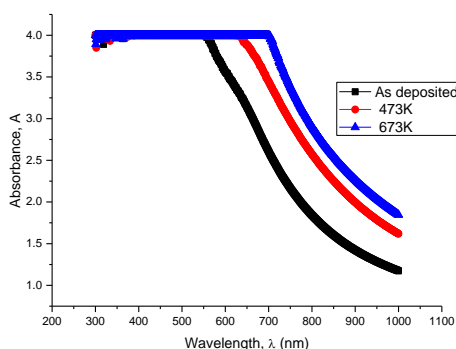
Fig. 4. Absorbance versus wavelength

From Fig.5, we deduce that the transmittance spectra change with increasing annealing temperature. It can be attributed to the change of thickness of the films and the scattering of incident light from the surface of the films due to the change of the grain size or an increase in the disorder of crystalline structure. The transmittance is generally low for all samples. This is due to the increase in crystalline size associated with higher densifications of the film. The figure also shows an improvement in transmittance of the film in the NIR region of the solar spectrum. The plots also show that in the UV and visible regions, samples exhibit low transmittance.
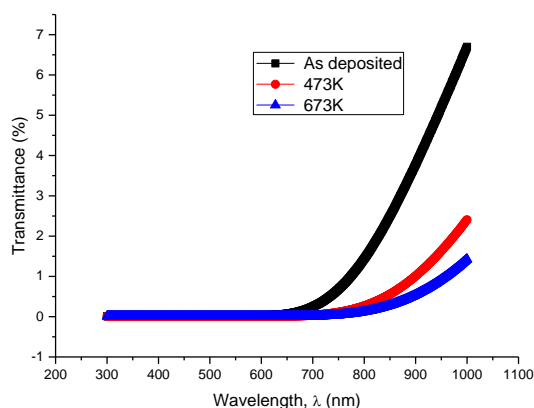
Fig. 5: Transmittance versus wavelength

The optical absorption of the prepared films has been studied in the range of (300- 1000 nm). The variation of optical density with wavelength is analyzed to find out the nature of transition, for different films were used to calculate the absorption coefficient (α) using the relation [10] α = 2.3026 A/t. Where A is the absorbance, and t is the film thickness. The variation of the absorption coefficient (α) as a function of photon energy (hν) is shown in Fig. 6.
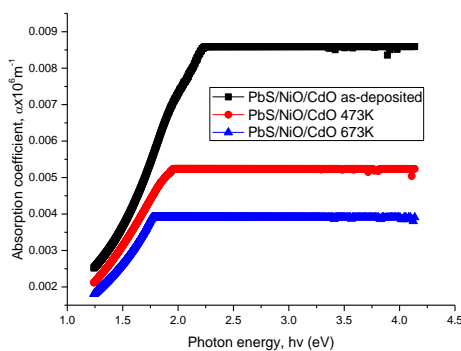
Fig. 6. Absorption coefficient versus photon energy

The absorption coefficient value decreased with the increase of the annealing temperature.

The energy band gap of the film was calculated by the following equation $(\alpha h v)^2 = A(h v - E_g)^n$ where , α , *h, v,* E_g and n are the absorption coefficient, a constant that depends on transition probability, Planck's constant, the frequency of the photons, optical band gap, and an index that characterizes the optical absorption process, respectively. n gets value of 1/2, 2, 3/2 or 3 for allowed direct, allowed indirect, forbidden direct and forbidden indirect transitions, respectively. In this study, the allowed direct band gaps of PbS-NiO-CdO thin film deposited at various annealing temperatures were determined by plotting $(\alpha h v)^2$ versus hν curves with the extrapolation of the linear region to low energies as shown in Figure 7. The allowed direct band gap of as-deposited is 1.70eV while annealed PbS-NiO-CdO thin film, the allowed direct band gap are 1.55eV and 1.38eV at temperatures 473K and 673K respectively. As a result of annealing, the energy band gap decreased from 1.70 eV to 1.38eV. This change in band energy is explained in terms of quantum confinement effect [11].
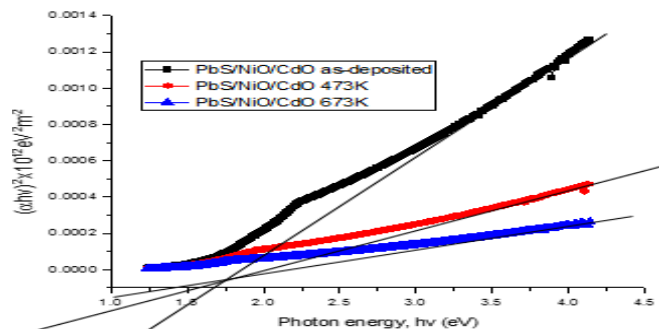
Fig. 7. Plot of (αhv)² versus photon energy

The decrease in optical band gap could be due to many body effects like the exchange energy due to electron-electron and electron-impurity interactions which occurs when the donor density exceeds a certain value and causes narrowing (red shift) of the band gap energy [12]. The decrease of the band gap can also be related to quantum confinement which has two consequences: First it splits the conduction band into discrete levels and secondly, it reduces the density of states available in the conduction band such that at 673K, the carrier concentration gets to its critical value leading to the collapse of the potential barrier at the grain boundaries and hence abrupt decrease in the optical band gap at 673K.

4. Conclusions

We have successfully deposited novel PbS/NiO/CdO heterojunction core-shell thin using chemical bath deposition technique. The structural, morphological and optical characteristics of film was discussed. The XRD patterns show that the film is polycrystalline in nature. SEM images depict the presence of both small and large grains. Spectrophotometric analysis enabled the estimation of the band gap of the film as 1.70eV, 1.55eV and 1.38eV for as deposited and annealed at 473K and 673K respectively.

Acknowledgement

References

[1] K. L. Chopra, "Thin-Film Solar Cells" Plenium Press, New York, Chapter **1**, 5 (1983).
[2] M. N. Nnabuchi, Optical, Solid state and Structural Characterization of Optimized Grown Thin films and their possible Applications in Solar Energy, PhD thesis, Department of Physics UNN, 18 (2004).
[3] S. M. Sze, Semiconductor Devices, Physics Technology, John Wiley and Sons New York, 9-45 (1981).
[4] P. E. Agbo, M. N. Nnabuchi, Chalcogenide Letters, **8** (4), 273 (2011).
[5] D. U. Onah, C. E. Okeke, F. I. Ezema, Asian Transactions on Science and Technology, **2**(1), 32 (2012).
[6] P. E. Agbo, G. F. Ibeh, S. O. Okeke, J. E. Ekpe, Communications in Applied Sciences **1**(1), 38 (2013).
[7] A. I. Onyia, M. N. Nnabuchi, Proceedings of the 1st African International Conferences/Workshop on Applications of Nanotechnology to Energy, Health and

Environment, UNN, March 23-29, 2014.

[8] D.U. Onah, E. I. Ugwu, J. E. Ekpe, American Journal of Nano Research and Applications, **3**(3), 62 (2015).

[9] M. Kavitha, M. Saroja, V. K. Romesh, G. Jenifer, International Journal of Thin Films Science and Technology **5**(2), 137 (2016).

[10] M. R. Islam and J. Podder, Cryst. Res. Technol. **44**, 286 (2009).

[11] R. N. Bhargava, D. Gallgher, X. Hong, A. Nurmikko, Phys. Rev. Lett. **72**, 416 (1994).

[12] N. Sharma, R. Kumar, Advances in Applied Science Research **5**(2), 111 (2014).